J|A|C|S
ARTICLES
Published on Web 03/09/2004

# Structure-Dependent Charge Transport and Storage in Self-Assembled Monolayers of Compounds of Interest in Molecular Electronics: Effects of Tip Material, Headgroup, and Surface Concentration

Fu-Ren F. Fan,[†] Yuxing Yao,[‡] Lintao Cai,[‡] Long Cheng,[‡] James M. Tour,*[,‡] and Allen J. Bard*[,†]

*Contribution from the Department of Chemistry and Biochemistry and Center for Nano- and Molecular Science and Technology, The University of Texas at Austin, Austin, Texas 78712-0165, and Department of Chemistry and Center for Nanoscale Science and Technology, Rice University, Houston, Texas 77005*

Received May 6, 2003; E-mail: ajbard@mail.utexas.edu

***Abstract:*** The electrical properties of self-assembled monolayers (SAMs) on a gold surface have been explored to address the relation between the conductance of a molecule and its electronic structure. We probe interfacial electron transfer processes, particularly those involving electroactive groups, of SAMs of thiolates on Au by using shear force-based scanning probe microscopy (SPM) combined with current−voltage ($i-V$) and current−distance ($i-d$) measurements. Peak-shaped $i-V$ curves were obtained for the nitro- and amino-based SAMs studied here. Peak-shaped cathodic $i-V$ curves for nitro-based SAMs were observed at negative potentials in both forward and reverse scans and were used to define the threshold tip bias, $V_{TH}$, for electric conduction. For a SAM of 2′,5′-dinitro-4,4′-bis(phenylethynyl)-1-benzenethiolate, **VII**, $V_{TH}$ was nearly independent of the tip material [Ir, Pt, Ir−Pt (20−80%), Pd, Ni, Au, Ag, In]. For all of the SAMs studied, the current decreased exponentially with increasing distance, $d$, between tip and substrate. The exponential attenuation factors ($\beta$ values) were lower for the nitro-based SAMs studied here, as compared with alkylthiol-based SAMs. Both $V_{TH}$ and $\beta$ of the nitro-based SAMs also depended strongly on the molecular headgroup on the end benzene ring addressed by the tip. Finally, we confirmed the "memory" effect observed for nitro-based SAMs. For mixed SAMs of **VII** and hexadecanethiol, **I**, the fraction of the charge collected in the negative tip bias region that can be read out at a positive tip bias on reverse scan (up to 38%) depended on the film composition and decreased with an increasing fraction of **I**, suggesting that lateral electron hopping among molecules of **VII** occurs in the vicinity of the tip.

## Introduction

Understanding how electrons flow through organic molecules is important in several areas: rationalizing electron transfer in organic and biological molecules; fabricating molecular electronic devices such as organic light-emitting devices (LED), memory devices, or field-effect transistors (FET); and developing single-molecule and single-electron devices.[1] One preferred approach for the assembly of molecules into devices and their connection to the macroscopic world relies on molecular self-assembly, such as self-assembled monolayers (SAMs).[2] Covalent attachment to metal or semiconductor surfaces can be achieved readily. Advances in modern synthetic supramolecular chemistry offer a huge range of molecular structures with different properties. Recent developments in device fabrication techniques and different experimental approaches allow single or a small group of molecules to be manipulated and investigated electronically.[3] Among them, solid-state metal−insulator−metal (MIM)[4] junction and scanning probe microscopy (SPM)[5] related techniques have frequently been used to study ultrathin films of organic materials.

Several groups have used SPM to probe tunneling across molecules in thin organic films.[6] By using conducting-probe AFM (CP-AFM),[7] Frisbie and co-workers measured $i-V$ curves for SAMs of alkanethiols on Au, and Rawlett and co-workers studied the negative differential resistance (NDR) effect[1] for

[†] The University of Texas at Austin.
[‡] Rice University.

(1) See, for example: Tour, J. M. *Molecular Electronics: Commercial Insights, Chemistry, Devices, Architecture and Programming*: World Scientific: New Jersey, 2003. Tour, J. M. *Acc. Chem. Res.* **2000**, *33*, 791, and references therein. Reed, M. A.; Tour, J. M. *Sci. Am.* **2000**, *282*, 86, and references therein. Chen, J.; Reed, M. A.; Rawlett, A. M.; Tour, J. M. *Science* **1999**, *286*, 1550. Xue, Y.; Datta, S.; Hong, S.; Reifenger, R.; Henderson, J. I.; Kubiak, C. P. *Phys. Rev. B* **1999**, *59*, R7852, and references therein.

(2) See, for example: Ulman, A. *Chem. Rev.* **1996**, *96*, 1533. Dubois, L. H.; Nuzzo, R. G. *Annu. Rev. Phys. Chem.* **1992**, *43*, 437. Finklea, H. O. In *Electroanalytical Chemistry*; Bard, A. J., Rubinstein, I., Eds.; Marcel Dekker: New York, 1996; Vol. 19, pp 110−335.

(3) See, for example: Cygan, M. T.; Jones, L., II; Allara, D. L.; Tour, J. M.; Weiss, P. S. *J. Am. Chem. Soc.* **1998**, *120*, 2721. Semaltianos, N. G. *Chem. Phys. Lett.* **2000**, *329*, 76.

(4) See, for example: Collier, C. P.; Mattersteig, G.; Young, E. W.; Luo, Y.; Beverly, K.; Sampaio, J.; Raymo, F. M., Stoddart, J. F.; Heath, J. R. *Science* **2000**, *289*, 1172.

(5) See, for example: *Scanning Tunneling Microscopy and Spectroscopy*, 2nd ed.; Bonnell, D. A., Ed.; VCH: New York, 2000. *Scanning Probe Microscopy*: *Analytical Methods*; Wiesendanger, R. Ed.; Springer-Verlag: Berlin, 1998.

molecules containing an electroactive nitro moiety.[8] Recently developed simplified models for electron tunneling across molecules in MIM junctions relate the current with distance, $d$, according to eq 1.[9]

$$i = i_0 \exp(-\beta d) \quad (1)$$

in which $\beta$ is a structure-dependent attenuation factor that was originally introduced to describe the extent of wave function mixing between the molecule and the two metal contacts.

Recently we reported results on the molecular electrical properties of SAMs of several compounds of interest in molecular electronics by using a tuning fork-based SPM technique combined with $i-V$ and $i-d$ measurements, for characterization and screening of compounds in an inert atmosphere.[10] We reported the effects of electroactive substituent groups on the central benzene ring of oligo(phenylene ethynylene)s (OPEs) and oligophenylenes (OPs) and the molecular wire backbone on their electric properties, and charge storage on nitro-based molecules.[10] In this paper we extend this earlier work and report systematic studies of interfacial electron transfer processes across SAMs of 2′-nitro-4,4′-bis(phenylethynyl)-1-benzenethiolate with different headgroups. We also studied the effect of different tip materials on electric conduction of SAMs of compound **VII**. In addition, we confirm the previously proposed model for charge storage in nitro-based SAMs by studies of mixed monolayers of **I** and **VII** that suggests that the "memory" effect we observed is mainly associated with lateral electron hopping rather than with the stochastic switching observed for metal/molecule junctions.[11]

## Experimental Section

**Materials.** The syntheses of the compounds (Chart 1) have been described elsewhere.[1,12] The gold substrate was prepared by cutting a single-crystal silicon wafer into a $6 \times 16$ mm$^2$ sheet, which was then cleaned for 30 min in a hot (40 °C), fresh acidic hydrogen peroxide (3:1 $H_2SO_4/H_2O_2$, v/v) solution. It was then rinsed with flowing distilled water, EtOH, and acetone and dried in flowing ultrahigh-purity $N_2$ gas. The gold films were deposited by thermal evaporation of 200 nm thick

***Chart 1.***

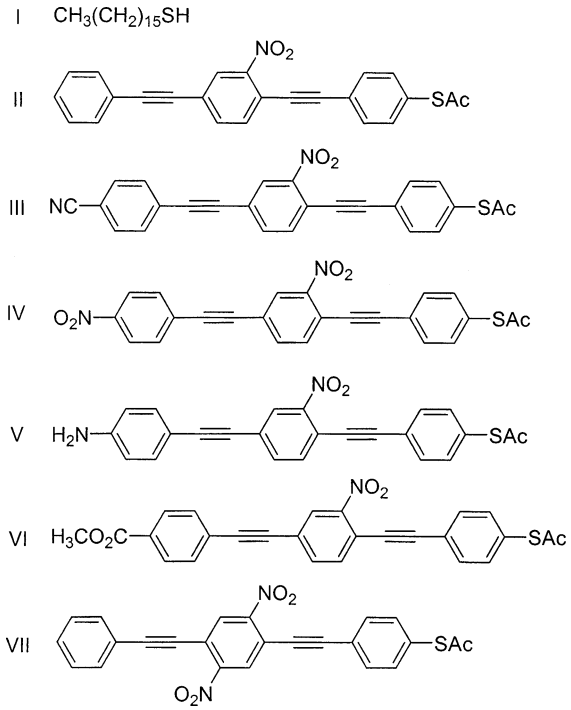


Au onto the Si sheets with a 25 nm Cr adhesion layer at a rate of 1 Å/s under a vacuum of $2 \times 10^{-6}$ Torr. The gold samples were finally stored in a $N_2$ atmosphere. Before use, the gold substrates were cleaned by a $UV/O_3$ cleaner (Boekel Industries, Inc., model 135500) for 10 min to remove organic contamination. After ultrasonic cleaning in EtOH for 20 min to remove the resulting gold oxide layer, the Au substrates were then rinsed with EtOH and acetone and then dried in flowing $N_2$. This procedure was confirmed to provide a clean, reproducible gold surface.[13]

Methylene chloride was distilled from calcium hydride. Tetrahydrofuran was distilled from sodium/benzophenone ketyl. All other chemicals were used as received without further purification.

**SAM Preparation.** SAMs were prepared by two reliable and reproducible methods: base promoted and acid promoted assemblies.[14] In the base-promoted technique, the compound (1 mg) was dissolved in a corresponding solvent, e.g., EtOH, THF, or a mixture of acetone/MeOH (2:1, v/v), in a 4 mL vial to a concentration of about 0.5 mM. Concentrated $NH_4OH$ (10 $\mu$L) was then added, and the mixture was incubated for 10 min to deprotect the thiolacetyl group. Addition of an excess of $NH_4OH$ (e.g., 40 $\mu$L) will lead to precipitation. A 200 $\mu$L sample of acetone/MeOH solution of 0.3 mM $Cs_2CO_3$ was also used for the deprotection. A clean gold substrate was then immersed into the solution at room temperature for a period of 20−24 h.

In the acid-promoted method, the compound (1 mg) was dissolved in a solvent mixture of $CH_2Cl_2$/MeOH (2:1 by volume) in a 4 mL vial. Concentrated $H_2SO_4$ (50−70 $\mu$L) was then added, and the solution was incubated for 1−4 h to deprotect the thiolacetyl moiety. A clean gold substrate was then immersed into the solution at room temperature for a period of 20−24 h. All the solutions were freshly prepared, previously purged with $N_2$ for an oxygen-free environment, and kept in the dark

(6) See, for example: Langlais, V. I.; Schittler, R. R.; Tang, H.; Gourdon, A.; Joachim, C.; Gimzeski, J. K. *Phys. Rev. Lett.* **2000**, *83*, 2809. Datta, S.; Tian, W.; Hong, S.; Reifenger, R.; Henderson, J. I.; Kubiak, C. P. *Phys. Rev. Lett.* **1997**, *79*, 2530. Zhou, S.; Liu, Y.; Xu, Y.; Hu, Z. D.; Qiu, X.; Wang, C.; Bai, C. *Chem Phys. Lett.* **1998**, *297*, 77. Donhauser, Z. J.; Mantooth, B. A.; Kelly, K. F.; Bumm, L. A.; Monnell, J. D.; Stapleton, J. J.; Price, D. W., Jr.; Rawlett, A. M.; Allara, D. L.; Tour, J. M.; Weiss, P. S. *Science* **2001**, *292*, 2303. Dunbar, T. D.; Cygan, M. T.; Bumm, L. A.; McCarty, G. S.; Burgin, T. P.; Reinerth, W. A.; Jones, L., II; Jackiw, J. J.; Tour, J. M.; Weiss, P. S.; Allara, D. L. *J. Phys. Chem. B* **2000**, *104*, 4880. Bumm, L. A.; Arnold, J. J.; Dunbar, T. D.; Allara, D. L.; Weiss, P. S. *J. Phys. Chem. B* **1999**, *103*, 8122.

(7) See, for example: Dai, H.; Wong, E. W.; Lieber, C. M. *Science* **1996**, *272*, 523. Alpersion, B.; Cohen, S.; Rubinstein, I.; Hodes, G. *Phys. Rev. B* **1995**, *52*, R17017. Klein, D.; McEuen, P. *Appl. Phys. Lett.* **1995**, *66*, 2478.

(8) Wold, D. J.; Frisbie, C. D. *J. Am. Chem. Soc.* **2000**, *122*, 2970. Kelley, T. W.; Granstrom, E. L.; Frisbie, C. D. *Adv. Mater.* **1999**, *11*, 261. Wold, D. J.; Frisbie, C. D. *J. Am. Chem. Soc.* **2001**, *123*, 5549. Rawlett, A. M.; Hopson, T. J.; Nagahara, L. A.; Tsui, R. K.; Ramachandran, G. K.; Lindsay, S. M. *Appl. Phys. Lett.* **2002**, *81*, 3043.

(9) See, for example: Ratner, M. A.; Davis, B.; Kemp, M.; Mujica, V.; Roitberg, A.; Yaliraki, S. *Ann. N. Y. Acad. Sci.* **1998**, *852*, 22. Segal, D.; Nitzan, A.; Davis, W. B.; Wasielewski, M. R.; Ratner, M. A. *J. Phys. Chem. B* **2000**, *104*, 3817.

(10) (a) Fan, F.-R. F.; Yang, J.; Dirk, S. M.; Price, D. W., Jr.; Kosynkin, D.; Tour, J. M.; Bard, A. J. *J. Am. Chem. Soc.* **2001**, *123*, 2454. (b) Fan, F.-R. F.; Yang, J.; Cai, L.; Price, D. W., Jr.; Dirk, S. M.; Kosynkin, D. V.; Yao, Y.; Rawlett, A. M.; Tour, J. M.; Bard, A. J. *J. Am Chem. Soc.* **2002**, *124*, 5550.

(11) Ramachandran, G. K.; Hopson, T. J.; Rawlett, A. M.; Nagahara, L. A.; Primak, A.; Lindsay, S. M. *Science* **2003**, *300*, 1413. Rawlett, A. M.; Hopson, T. J.; Nagahara, L. A.; Tsui, R. K.; Ramachandran, G. K.; Lindsay, S. M. *Appl. Phys. Lett.* **2002**, *81*, 3043.

(12) Allara, D. L.; Dunbar, T. D.; Weiss, P. S.; Bumm, L. A.; Cygan, M. T.; Tour, J. M.; Reinerth, W. A.; Yao, Y.; Kozaki, M.; Jones, L., II. *Annal. N.Y. Acad. Sci.* **1998,** *852*, 349. Chen, J.; Wang, W.; Reed, M. A.; Rawlett, A. M.; Price, D. W.; Tour, J. M. *Appl. Phys. Lett.* **2000**, *77*, 1224. Tour, J. M.; Kozaki, M.; Seminario, J. M. *J. Am. Chem. Soc.* **1998**, *120*, 8486. Sonogashira, K. In *Metal-catalyzed Cross-Coupling Reactions*; Diederich, F., Stang, P. J., Eds.; Wiley-VCH: New York, 1998; pp 203−230.

(13) Ron, H.; Matlis, S.; Rubinstein, I. *Langmuir* **1998**, *14*, 1116. Ron, H.; Rubinstein, I. *J. Am. Chem. Soc.* **1998**, *120*, 13444.

(14) Cai, L.; Yao, Y.; Price, D. W.; Tour, J. M. *Chem. Mater.* **2002**, *14*, 2905.

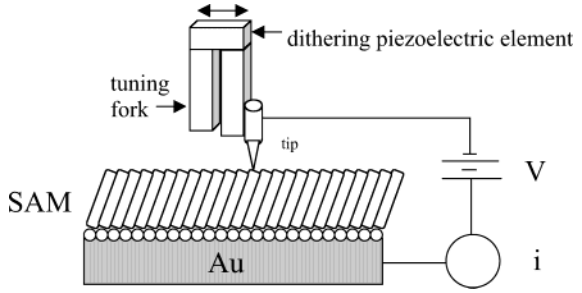


***Figure 1.*** Schematic representation of the measurement and formation of a MIM junction with a tuning fork-based SPM tip containing a SAM on Au.

during immersion to avoid photo-oxidation. After the assembly, the samples were removed from the solutions, rinsed thoroughly with methanol, acetone, and $CH_2Cl_2$, and finally blown dry with $N_2$. Usually the SAMs of compounds **IV** and **VII** were prepared under acidic conditions, while the others were prepared using the basic condition.

Mixed SAMs consisting of compounds **I** and **VII** were prepared by immersing clean Au substrates in mixed solutions containing the two molecules at different ratios for a period of 18 h. Compound **VII** was deprotected by the acid-promoted method as described above before mixing with the molecule **I**.

**Apparatus and Measurements.** Monolayer thickness was determined using either a Rudolph series 431A ellipsometer or a Gaertner LSE ellipsometer. The He-Ne laser (632.8 nm) light was incident at 70° on the sample. Measurements were carried out before and immediately after monolayer adsorption. The length of the molecular wire was calculated from the sulfur atom to the furthest proton for the minimum energy extended forms by molecular mechanics. As reported by Tour et al.,[15] an $n_f$ value of 1.55 and $k_f = 0$ were assumed for all the film thickness calculations and the Au−S−C bond angle was assumed to be linear at 0.24 nm for the Au−S bond length. The OPE system has a tilt angle of the long molecular axis of <20° from the normal to the substrate surface, which will give a maximum of ~6% decrease in thickness as compared to that calculated on the basis of a vertical linear Au−S−C bond angle. The variation of this calculated thickness is less than the error in the ellipsometric measurement (5−10%). Sabataniet al.[16] also assumed that all thioaromatic monolayers studied had an $n_f$ of 1.5 and were transparent ($k_f = 0$ at wavelength 632.8 nm) and that the original refractive index of gold substrate was not altered by the adsorbed layer. A variation of $n_f$ between 1.4 and 1.6 does not significantly change the thickness measured.

The principle of this experiment is shown in Figure 1. Electrical contact to one side of the SAM was made directly by the Au layer. The $i-V$ and $i-d$ curves were measured with a tuning fork-based SPM[17] constructed on the basis of the procedures reported previously by Karrai and Grober.[18] A constant current suppression of a few tenths of pA was sometimes used to correct for the offset of the current amplifier. A sharpened metal (Ir, Pt, Ir−Pt (20−80%), Pd, Au, Ag, or Ni) wire (100−500 $\mu$m diameter) serving as the tip is glued along the side of one of the prongs of a quartz crystal tuning fork. An In tip was grown on a sharpened Ir−Pt tip by immersing and then pulling it slowly from a molten indium drop. The indium-coated tip was then examined under an optical microscope. Indium dendrites located near the very end of the tip can be obtained with a low, but acceptable, success rate, but we rarely obtained a single indium dendrite at the very end of the Ir−Pt tip. The mechanical resonance of the fork is excited with a piezoelectric tube, which served the purpose of dithering where the tuning fork and the tip are vibrated parallel to the sample surface. When the tip just contacts the SAM surface, the amplitude and frequency of the oscillation decrease, and this can be used to sense the presence of the surface. Thus, the tip can be moved to the substrate and positioned fairly rapidly. The tip is then retracted slightly (~10−20 nm) and moved to a different location on the SAM. The SPM is then operated in the current-measurement mode as a function of voltage or distance with the feedback loop turned off. The $i-V$ curves were obtained by sweeping the potential of the tip with respect to the Au substrate at a scan rate of 6 V/s over the desired potential range and recording the current, as the tip again approached toward the SAM, this time in small steps (1.0−3.5 Å each step). We measured the current that flowed across the SAM in response to changes in bias voltage while the tip approached stepwise toward the surface of a SAM on Au. Before the tip contacts the molecules in the SAM, essentially no current in excess of the noise level (~0.2 pA) flowed. The constant background current observed during voltage scan is mainly associated with the capacitive charging of the system. When a current greater than a few times the noise level flowed across the SAM, the first and several subsequent $i-V$ curves were recorded. The $i-d$ curves were obtained by biasing the tip at a fixed potential and approaching it slowly (~10 Å/s) toward the surface of a SAM and measuring the current flowing through the junction as a function of tip displacement. All measurements were carried out at room temperature (25.0 ± 0.5 °C) under dried argon in the dark.

## Results and Discussion

Electron transport across metal tip−SAM−metal junctions depends strongly on the position of the Fermi level of the metal electrodes relative to the lowest unoccupied molecular orbital (LUMO) and the highest occupied molecular orbital (HOMO) of the molecular bridge. When the difference in energy between the LUMO and the Fermi level is large, electron transport occurs by superexchange,[9] i.e., electron tunneling mediated by interaction between two contacts and unoccupied orbitals of the organic bridge separating them. In this case, the current increases exponentially with decreasing distance and is characterized by a relatively large $\beta$ value; For example, $\beta$ values of 1.1−1.4 $Å^{-1}$ for SAMs of alkylthiols[6,8,10] have been measured by SPM techniques and discussed extensively and will not be considered further here. When the Fermi level approaches the energy of the molecular orbital of the molecular bridge, a "resonance" effect can take place and the conduction of electrons will occur through the MOs, which are affected by interaction with the contacts and with the applied voltage.[9,19,20] In this case, the current is less distance-dependent and the $i-V$ characteristic depends strongly on the molecular structure. We will focus on the latter case in the following discussion, especially of those SAMs containing electroactive nitro- or amino-based substituent groups that can act as an electron or hole "trap".[10]

**(a) Effect of Headgroups and Tip Materials at the Tip/SAM Interface on $V_{TH}$.** The nature of the electronic contact to the molecules is important in both conventional and single-molecule devices,[21] as well as in organic LEDs and FETs. The interfacial energetics need to be considered. For a molecular wire, the anchoring and headgroups chosen should form an ohmic, i.e., barrierless, contact at the (SAM/contact) interface.

(15) Tour, J. M.; Jones, L.; Pearson, D. L.; Lamba, J. J. S.; Burgin, T. P.; Whitesides, G. M.; Allara, D. L.; Parikh, A. N.; Atre, S. *J. Am Chem. Soc.* **1995**, *117*, 9529,
(16) Sabatani, E.; Cohen-Boulakia, J.; Bruening, M.; Rubinstein, I. *Langmuir* **1993**, *9*, 2974.
(17) Fan, F.-R. F.; Bard, A. J. *J. Electrochem. Soc.* **1989**, *136*, 3216.
(18) Karrai, K.; Grober, R. D. *Appl. Phys. Lett.* **1995**, *66*, 1842.
(19) Seminario, J. M.; Zacarias, A.; Tour, J. M. *J. Am. Chem. Soc.* **2000**, *122*, 3015.
(20) Datta, S. *Electronic Transport in Mesoscopic Systems*; Cambridge University Press, 1995. Damle, P. S.; Ghosh, A. W.; Datta, S. *Phys. Rev. B Rapid Commun.* **2001**, *64*, R201403.
(21) Cui, X. D.; Primak, A.; Zarate, X.; Tomfohr, J.; Sankey, O. F.; Moore, A. L.; Moore, T. A.; Gust, D.; Harris, G.; Lindsay, S. M. *Science* **2001**, *294*, 571. Hipps, K. W. *Science* **2001**, *294*, 536. Cui, X. D.; Primak, A.; Zarate, X.; Tomfohr, J.; Sankey, O. F.; Moore, A. L.; Moore, T. A.; Gust, D.; Nagahara, L. A.; Lindsay, S. M. *J. Phys. Chem. B* **2002**, *106*, 8609.

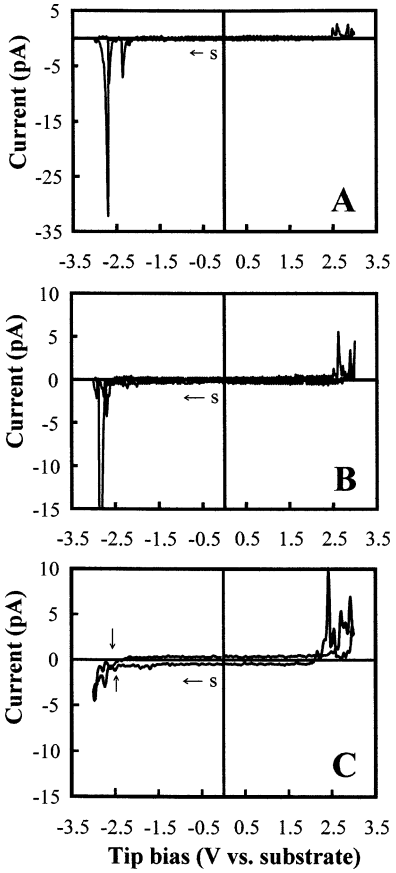


***Figure 2.*** Typical first $i-V$ curves for compounds **II** (curve A), **III** (curve B), and **V** (curve C) when the Pt tip barely touched the surface of SAMs on Au. Tip voltage (vs Au substrate) was scanned first from 0 to the negative limit, back to 0, then to the positive limit and finally stopped at 0 V. S → stands for the starting point of the voltage scan (usually 0 V) and the initial scan direction. The double vertical arrows in curve C show where the first negative $V_{TH}$ values are located in the forward and reverse scans.

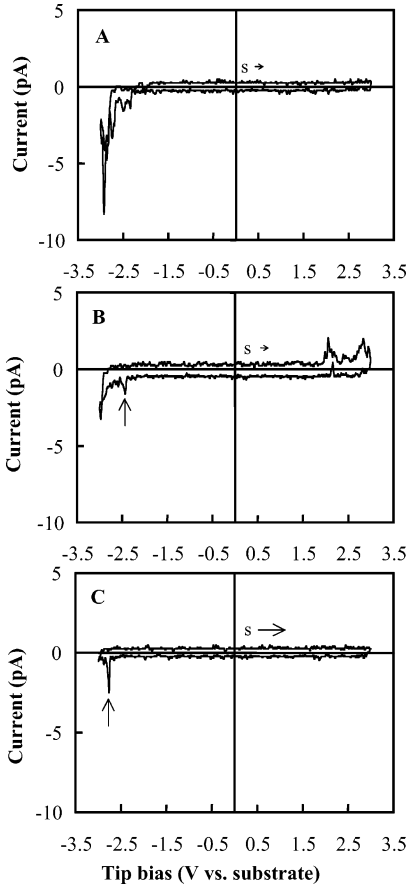


***Figure 3.*** Typical first $i-V$ curves for compounds **III** (curve A), **V** (curve B), and **VI** (curve C) when the Pt tip barely touched the surface of SAMs on Au. Tip voltage (vs Au substrate) was scanned from 0 to the positive limit, back to 0, then to the negative limit and finally stopped at 0 V. S → stands for the starting point of the voltage scan (usually 0 V) and the initial scan direction. The vertical arrows in curves B and C show the location of the first negative $V_{TH}$.

However, for a molecular memory device, the introduction of a proper anchoring group at the (SAM/substrate) interface or a functional headgroup at the other interface may allow the creation of a barrier that leads to the MO localization that is required for the device to function.

We have previously[10] briefly addressed the effects of the anchoring group at the (substrate/SAM) interface on the electric behavior of OPE or OP backbone-based SAMs. For nitro-based OPs or OPEs, e.g., a SAM of 2′,5′-dinitro-4,4′-bis(phenylethynyl)-1-benzenethiolate, **VII**, reversible peak-shaped $i-V$ curves could be obtained (see **Supporting Information**). The peak positions show small variations (±0.1 V) in position that are nearly independent of the current amplitudes; the latter show much more significant fluctuations among the different scans due to the gap variation and the strong distance dependence of the current. The peak positions were characteristic of the particular OPE and were potential dependent. The positions were clearly not random and thus were not caused by stochastic events, as sometimes seen in STM scans of similar films.

We address here first the effect of the headgroup at the end benzene ring of 2′-nitro-4,4′-bis(phenylethynyl)-1-benzenethiolate, **II**, on its electric properties. Figure 2A shows one $i-V$ curve when a Pt tip barely touched the surface of a SAM of **II** on an Au substrate. The current through the film correspondsto the onset of conduction of the molecule. As shown, when the negative scan reached about −2.3 V, a current peak of a few pA was observed. We define this peak potential as the threshold tip bias ($V_{TH}$) for electrical conduction. This $i-V$ curve also clearly showed at least one additional current peak in the negative bias region, which is probably related to the redox activity of the compound. With **II**, an initial scan to positive tip bias at a fresh location did not show significant current in the voltage range of 0−3 V (not shown). This demonstrates the rectifying behavior in the electric conduction of a fresh SAM of molecules bearing reducible nitro-substituent groups. Notice, however, that anodic current peaks appeared after the tip was first scanned to negative bias (see Figure 2A). We refer to this behavior as the "memory" effect. When the headgroup H atom of the end benzene ring of **II** was replaced with either a strong electron-withdrawing (reducible) cyano (or nitro) group or a strong electron-donating (oxidizable) amino group, the shape of the $i-V$ curve changed considerably. As shown in Figure 2B for **III**, a cyano headgroup enhanced peak heights at positive tip bias after the tip was first scanned to negative potentials. A similar effect (data not shown) was also observed for a nitro headgroup, **IV**. In these cases, the current at positive tip bias < 3 V is associated with a reoxidation process following the negative scan reduction process, since an initial scan to positive tip bias at a fresh location did not show significant peaks in this voltage range (compare the current at positive tip bias in Figure 3A with that in Figure 2B for a reference current at the

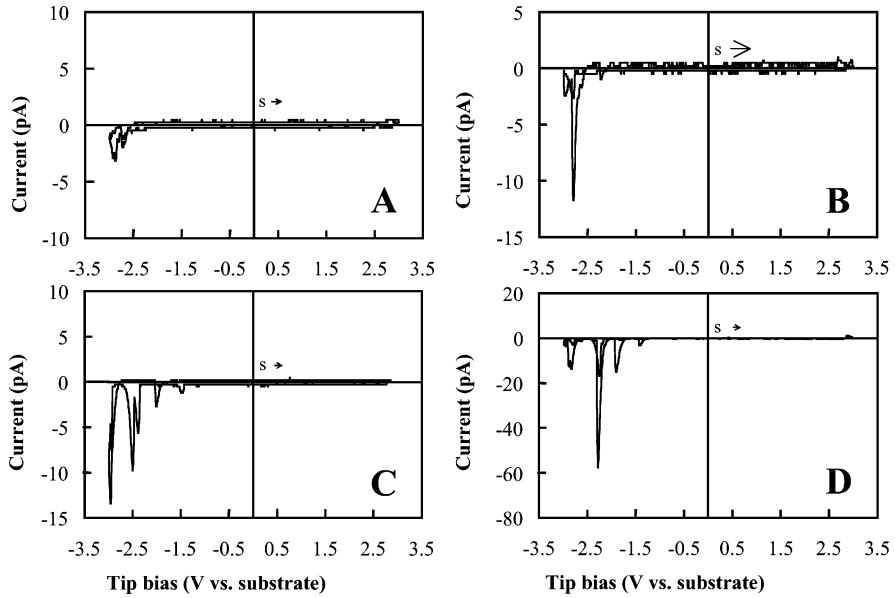


***Figure 4.*** Representative $i-V$ curves for compound **VII** with different tip materials: curve A for In, curve B for Ni, curve C for Ag, and curve D for Au. Tip voltage (vs Au substrate) was scanned from 0 to the positive limit, back to 0, then to the negative limit and finally stopped at 0 V. S → stands for the starting point of the voltage scan (usually 0 V) and the initial scan direction.

***Table 1.*** Threshold Tip Bias ($V_{TH}$) for Several Compounds[a,b]

| compound | headgroup | first negative peak voltage,[c] V | first positive peak voltage,[d] V |
|---|---|---|---|
| **II** | $-H$ | $-2.30 \pm 0.10$ | |
| **III** | $-CN$ | $-2.20 \pm 0.06$ | |
| **IV** | $-NO_2$ | $-1.56 \pm 0.15$ | |
| **V** | $-NH_2$ | $-2.45 \pm 0.10$ | $+2.18 \pm 0.18$ |
| **VI** | $-CO_2CH_3$ | $-2.79 \pm 0.05$ | |
| **VII** | | $-1.75 \pm 0.10$ | |

[a] $V_{TH}$ values are taken as the average of 5−25 $i-V$ curves with different Pt tips at different locations for each compound (standard deviation shown). Only peaks showing a signal-to-background noise ratio of greater than 2 were used. [b] SAMs of **V** and **VI** are prepared by the base-deprotected technique and the rest by the acid-deprotected method. [c] Negative tip bias scans at locations never previously scanned into the negative voltage regime. [d] Positive tip bias scans at locations never previously scanned into the positive or negative voltage regime.

negative bias) for **III**. Notice that we can only discuss the enhancement of the reoxidation current on a relative basis, since the absolute peak heights are strongly dependent on the tip/substrate distance, which varied in different scans. When the head hydrogen atom of the end benzene ring of **II** was replaced with an oxidizable amino group to form **V**, electric current peaks at positive tip bias became more prominent as compared with that at negative tip bias (see Figure 2C). Notice also that with **V**, unlike **II** and **III**, an initial scan to positive tip bias at a fresh location showed some significant peaks at about 2.1 and 2.8 V and one current peak near ca. −2.45 V in the reverse negative bias region (see Figure 3B). When the head hydrogen atom was replaced with a blocking $-COOCH_3$ group, as shown in Figure 3C for **VI**, no current flowed in the positive tip bias region and the negative $V_{TH}$ shifted to a more negative value ($V_{TH} = -2.79$ V) as compared with **II** ($V_{TH} = -2.3$ V). We summarize the first negative and positive $V_{TH}$ values of several compounds in Table 1.

Second, we studied the effect of tip material on the electrical behavior of a SAM of 2′,5′-dinitro-4,4′-bis(phenylethynyl)-1-benzenethiolate, **VII**, on Au. This is important if we are to understand how to decrease the barrier height for charge

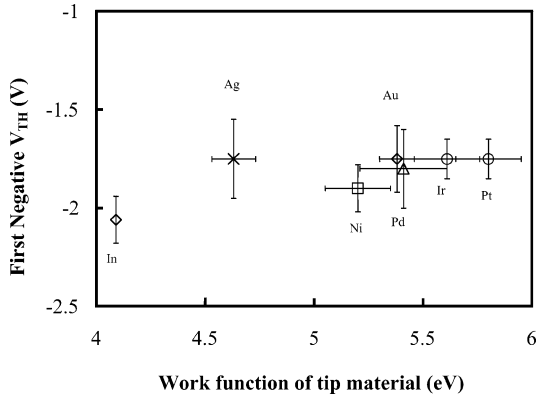


***Figure 5.*** First negative threshold tip bias, $V_{TH}$, for **VII** vs the work function of tip material. $V_{TH}$ is the average of 7−25 $i-V$ curves for each kind of tip material with the same film but measured at different locations (standard deviation shown). Notice that those metals that tend to form insulating surface oxide layers, such as indium and nickel, show smaller current flows and slightly more negative $V_{TH}$ values, i.e., correspond to a larger electron injection barrier height.

injection, since the electrical behavior of monolayers can be dominated by parasitic potential drops across the interfaces. We chose several different metals, ranging from indium (work function ∼4.1 eV) to iridium (work function 5.6 ± 0.2 eV),[22] as tip materials. Typical $i-V$ curves are shown in Figure 4, and the first negative $V_{TH}$ values are summarized in Figure 5. As shown, the first $V_{TH}$ values were nearly independent of tip material, although those that tend to form insulating surface oxide layers, such as indium and nickel, showed smaller current flows and slightly more negative $V_{TH}$ values, i.e., a corresponding larger electron injection barrier height. Notice that in the same potential range studied the number of cathodic current peaks observed with In and Ni tips were fewer than seen with precious metal tips mainly due to the reduced current. The lack

(22) Hölzl, J.; Schulte, F. K Work Functions of Metals. In *Solid State Physics*; Höhler, G. Ed.; Springer-Verlag: Berlin, 1979. Riviere, J. C. Work Function: Measurements and Results. In *Solid State Surface Science*; Green, M., Ed.; Decker: New York, 1969; Vol. 1. Miachaelson, H. B. *J. Appl. Phys.* **1977**, *48*, 4729.

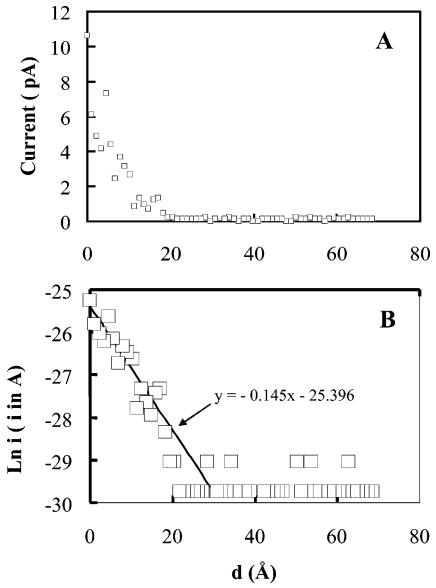


***Figure 6.*** Typical (current vs tip displacement) curves at +3.0 V tip bias (vs substrate) for a SAM of compound **V** on Au: (A) in a linear scale; (B) in a semi-natural logarithmic scale.

of correlation between $V_{TH}$ of **VII** and the work function of the tip material is strikingly different from the experimental results on superexchange for aliphatic SAMs[23] where the interaction between the metal contact and the molecule is weak, as well as with theoretical predictions where the electric conduction is assumed to be mainly via a delocalized MO simultaneously connecting the molecule to the contact electrodes at both ends.[24] However, our results do not exclude the possibility that under our experimental conditions there might be localized MOs that allow electron hopping from the tip to those MOs and then from there to the substrate, analogous to some electron transfer reactions on electrochemically inert electrodes (see discussions below).

**(b) Distance Dependence of Film Conductance.** Third, we explored the electrical behavior of a SAM as a function of tip/Au substrate distance at a fixed bias. For all SAMs studied, the current increased exponentially as the tip penetrated the monolayer with decreasing gap, *d*, between tip and Au substrate according to an empirical relation of the form of eq 1. Typical current versus distance ($i-d$) curves for compound **V** at +3.0 V tip bias (versus substrate) are shown in Figure 6. The $d = 0$ position indicates where the tunneling current increases sharply as the tip touches the gold. In Table 2, we summarize these empirical $\beta$ values for different SAMs and tip materials at a tip bias of either −3.0 or 3.0 V. As shown, with a Pt tip, the nitro-based SAMs show low $\beta$ values, ranging from 0.34 Å$^{-1}$ for **VII** to 0.50 Å$^{-1}$ for **III** as compared to hexadecanethiol (1.37 Å$^{-1}$, as reported in ref 10) at −3.0 V tip bias. The SAM with an amino headgroup, **V**, had the lowest $\beta$ value of 0.16 Å$^{-1}$ at a tip bias of 3.0 V. Compounds **IV** and **VII** showed similar $\beta$ values, although the addition of a nitro headgroup (compound **IV**) shifted $V_{TH}$ substantially positive as compared to **VII**. Notice also that, similar to the behavior of $V_{TH}$, the $\beta$ value of **VII** at a −3.0 V tip bias was nearly independent of the tip material.

***Table 2.*** $\beta$ Values of Some Compounds as a Function of Tip Material and Bias (with respect to Au substrate)[a]

| compound | tip material | $\beta$ at − 3.0 V, Å$^{-1}$ | $\beta$ at + 3.0 V, Å$^{-1}$ |
|---|---|---|---|
| **III** | Pt | 0.50 ± 0.09 | |
| **IV** | Pt | 0.38 ± 0.03 | |
| **V** | Pt | | 0.16 ± 0.02 |
| **VI** | Pt | 0.44 ± 0.06 | |
| **VII** | Pt | 0.34 ± 0.03 | |
| **VII** | Ir | 0.33 ± 0.03 | |
| **VII** | Ni | 0.31 ± 0.02 | |
| **VII** | Au | 0.32 ± 0.04 | |
| **VII** | Ag | 0.26 ± 0.03 | |
| **VII** | In | 0.30 ± 0.02 | |

[a] The average of 5−15 points with standard deviation shown.

Thus, the $\beta$ values reported here seem to reflect some relation between the molecular electrical properties and the electronic structure of the molecules. A theoretical model that relates molecular structure to molecular electrical behavior would be very helpful for interpreting these $\beta$ values.

Furthermore, interfacial energetics is not the only factor to consider in charge transport through a molecule. Both electronic coupling and charge and nuclear-coordinate relaxation dynamics are also important.[25,26] During the passage of an electron through a molecule, the strong electric field effect may lead to the formation of a molecular polaron[27] or localized MOs,[28] when a strong electron-accepting or electron-donating group is present. This might account for the existence of a long-lived "radical anion" state that permits "charge trapping", which is discussed in the following section. Even after the decay of the molecular polaron or radical ion, the resulting excitation in nuclear coordinates, as well as environmental effects (e.g., from contact pressure)[29] and thermal fluctuations, may lead to meta-stable structural or conformational changes to produce the "switching" behavior.[30]

**(c) Charge Storage and Lateral Electron Hopping.** An important issue with these kinds of films in connection with the possible construction of memory devices is the elucidation of the mechanism of the "memory" effect. In our earlier paper we proposed that one mechanism involves lateral hopping of charge in the film, in addition to the resonant tunneling through the molecular chains to the Au substrate (see Scheme 1 and Figure 11 in ref 10b). Here we provide additional experiments that support this charge storage mechanism observed for nitro-based SAMs[10] and demonstrate that this effect is a function of the composition of a mixed SAM of compounds **I** and **VII**. As shown in Table 3, the thickness of mixed SAMs is essentially independent of their composition and the nature of the substrate (Si or glass) on which the Au and SAM are deposited. As with the previously described $i-V$ measurements, the tip bias was scanned negatively from 0 to −3.0 V and then back to 0 V with the tip barely touching the surface

(23) Beebe, J. M.; Engelkes, V. B.; Miller, L. L.; Frisbie, C. D. *J. Am. Chem. Soc.* **2002**, *124*, 11268.
(24) Seminario, J. M.; De La Cruz, C. E.; Derosa, P. A. *J. Am. Chem. Soc.* **2001**, *123*, 5616.
(25) Kuznetsov, A. M.; Ulstrup, J. *J. Inclus. Phenom. Macrocy. Chem.* **1999**, *35*, 45.
(26) Cornil, J.; Karzazi, Y.; Bredas, J. L. *J. Am. Chem. Soc.* **2002**, *124*, 3516.
(27) Silinsh, E. A.; Capek, V. *Organic Molecular Crystals*: *Interaction, Localization, and Transport Phenomena*; AIP Press: Woodbury, 1994.
(28) Bredas, J. L. and co-worker, private communication.
(29) See, for example: Lang, H. P.; Thommen-Geiser, V.; Guentherodt, H. J. *Synth. Met.* **1996**, *77*, 161. Joachim, C.; Gimzewski, J. K. *Proc. IEEE* **1998**, *86*, 184. Son, K. A.; Kim, H. I.; Houston, J. E. *Phys. Rev. Lett.* **2001**, *86*, 5357.
(30) Donhauser, Z. J.; Mantooth, B. A.; Kelly, K. F.; Bumm, L. A.; Monnell, J. D.; Stapleton, J. J.; Price, D. W. Jr.; Rawlett, A. M.; Allara, D. L.; Tour, J. M.; Weiss, P. S. *Science* **2001**, *292*, 2303.

***Table 3.*** Thickness and $Q_a/Q_c$ Values of Mixed SAMs of **I** and **VII** Prepared by the Acid-Deprotected Method

| mol % of **VII**[a] | substrate[b] | thickness, nm | $Q_a/Q_c$ (=$Y$)[c] |
|---|---|---|---|
| 100 | Au/Si | 2.1 | 0.38 ± 0.04 |
| 100 | Au/glass | 2.3 | 0.38 ± 0.04 |
| 95 | Au/Si | 2.3 | 0.37 ± 0.06 |
| 91 | Au/Si | 2.3 | 0.33 ± 0.04 |
| 75 | Au/glass | 2.2 | 0.25 ± 0.04 |
| 60 | Au/glass | 2.1 | 0.13 ± 0.03 |
| 50 | Au/Si | 2.1 | 0.10 ± 0.04 |
| 40 | Au/glass | 1.5 | N.A. |
| 33 | Au/Si | 2.1 | 0.05 ± 0.03 |
| 25 | Au/glass | 2.2 | 0.05 ± 0.03 |
| 9 | Au/Si | 2.3 | 0.02 ± 0.02 |
| 0 | Au/glass | 2.4 | N.A. |
| 0 | Au/Si | 2.2 | N.A. |

[a] Composition of the solutions for SAM preparation. [b] 20−25 nm Cr adhesion layer was used between Au (160−200 nm thick) and Si or glass substrate. [c] The average of 5−10 scans with standard deviation shown.

of SAM. With or without an intermittent delay, $t_d$, the tip was then scanned to positive potentials several times from 0 to +3.0 and then back to 0 V. The ratio $Q_a/Q_c = Y$, where $Q_c$ is total charge in the peaks in the negative bias region and $Q_a$ is in the positive bias region after the negative scan, was calculated. $Q_a$ and $Q_c$ were obtained by integrating the current (after the correction for the background current) with respect to time under the current peaks in the anodic or cathodic bias region. Figures 7B and 7C show two consecutive positive scans for an acid-promoted mixed SAM of **VII** and **I** (mole ratio **VII**:**I** = 3:1 in the solution for SAM preparation)[31] from 0 to +3.0 V at the same spot after a single initial negative tip scan from 0 to −3.0 V with $t_d = 0$ s (see Figure 7A). All three curves were recorded at the same tip−substrate distance. For clarity, we show only the forward scans of the $i-V$ curves. As shown, while current peaks were observed in the first positive scan after the initial negative scan, these disappeared in a subsequent positive scan. These results demonstrate the memory effect of these nitro-based SAMs. The value of $Q_a/Q_c$ for this mixed SAM with $t_d = 0$ s is ∼0.25 as compared to ∼0.38 for a SAM of pure **VII**. The normalized $Q_a/Q_c$ values, $Y/Y_0$ (where $Y_0 = (Q_a/Q_c)_{X=1} = 0.38$), as a function of mole fraction, $X$, of **VII** are summarized in Figure 8. As shown, when $X$ is less than ∼0.4, this ratio is small, and it increases with larger values of $X$ according to the approximate relation

$$Y/Y_0 = (X - 0.34)^{1.2} \qquad (2)$$

This "percolation-like" composition-dependent relation suggests that the charge storage phenomenon observed here for **VII** involves an electric conduction process of dimensionality greater than 1. More specifically, it is consistent with a lateral electron-hopping process along the SAM plane from the localized MOs to the vicinity of the tip−contact area. Charges localized under the tip will mainly tunnel to the substrate, so as $X$ goes to 0, no charge will be stored. With lateral electron hopping, more charges will move away from the tip location to the near neighborhood with a greater amount of the "conductive" nitro molecule, **VII**. This favors a larger relative amount of charge available for read-out. As the surface concentration of the nitro compound is diluted with the alkylthiol, the probability of lateral charge transport decreases. Consistent with this result, we also observed that $Q_a/Q_c$ decreases as the delay time between the end of the negative sweep and the start of the positive one, $t_d$, increases. For a SAM of pure **VII**, $Q_a/Q_c$ decreased from ∼0.38 for $t_d = 0$ s to ∼0.25 for $t_d = 0.2$ s to <0.05 for $t_d = 2$ s. With the feedback loop off, we can only carry out experiments with

(31) Voltammograms of mixed SAMs of **I** and **VII** in acetonitrile containing 0.1 M tetrabutylammonium fluoroborate show two reduction waves at halfwave potentials of about −0.69 and −0.92 V vs sodium SCE (SSCE). The heights of the waves are nearly proportional to the molar fraction, $X$, of **VII** in the solution for SAM preparation when it is greater than 0.5. Those waves are less clear when $X$ is smaller than 0.4. Electrochemistry of these kinds of compounds dissolved in solution or prepared as SAMs is currently under investigation, and detailed results will be reported elsewhere.

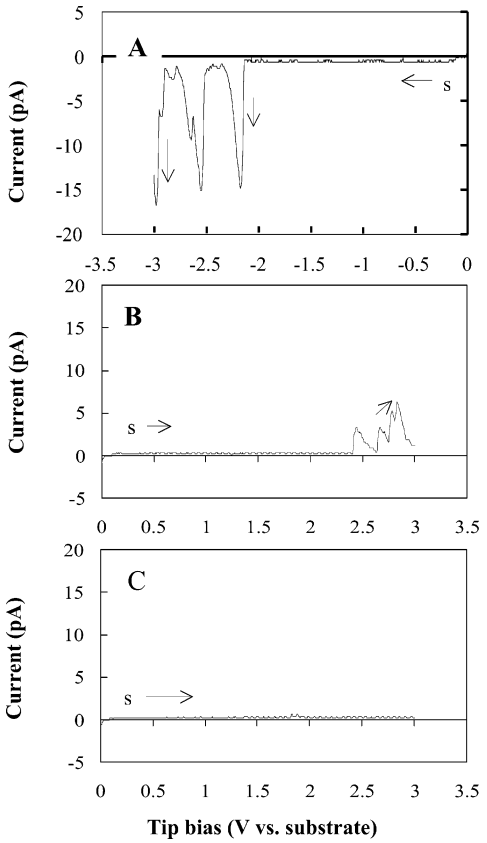


***Figure 7.*** (A) Single $i-V$ curve at a Pt tip for an initial negative tip scan from 0 to −3.0 V for an acid-promoted mixed SAM of **VII** and **I** (mole ratio **VII**:**I** = 3:1 in the solution for SAM preparation). (B and C) Two consecutive positive scans from 0 to +3.0 V after the initial negative scan A ($t_d = 0$ s). For clarity, only forward scans are shown. S → stands for the starting point of the voltage scan (usually 0 V) and the scan direction.

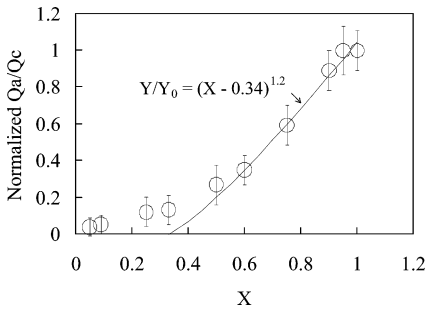


***Figure 8.*** Normalized $Q_a/Q_c$ ($Y/Y_0$) for mixed SAMs of **I** and **VII** as a function of mole fraction, $X$, of **VII** in the solutions for their preparation. $Q_c$ and $Q_a$ are the total charges in the peaks in the negative and positive bias regions, respectively. Symbols are experimental data, and the line is the fitting above a threshold $X = 0.34$ based on eq 2.

$t_d$ of only a few seconds because of thermal drift of the tip. Notice that in any case, $Q_c$ is substantially greater than $Q_a$ in magnitude, suggesting that the resonant tunneling down the molecular chains beneath the tip is still a dominant process as compared to the lateral electron hopping.

## Conclusions

From these experiments, we conclude that the molecular conductance depends strongly on the structure of the molecules, e.g., the nature of the electroactive headgroup (at the end benzene ring of **II)**. We show that the first negative or positive $V_{TH}$ depends strongly on the headgroup. The first negative $V_{TH}$ ranges from ca. −1.7 V for dinitro compound, **VII**, to ca. −2.8 V for **VI**. The introduction of an oxidizable amino group as the headgroup of the end benzene ring of **II** favors the electric conduction at positive tip bias as compared to a negative one, and in this case, we can observe relatively significant positive current without scanning the tip to a negative bias first. These experiments demonstrate not only the NDR effect but also the rectifying behavior of the electric conduction of a fresh SAM of these molecules. We confirmed the memory effect observed for nitro-based molecules. The experimental results on the memory effect of the mixed SAMs of **I** and **VII** suggest that lateral electron hopping is significant and this lateral "cross talk" between individual molecular wires is important in the design of molecular electronic devices.

**Acknowledgment.** The support of this work by the National Science Foundation, CHE0202136, the Defense Advanced Research Projects Agency, the Office of Naval Research, and Molecular Electronics Corp. is gratefully acknowledged.

**Supporting Information Available:** A figure demonstrating the reproducibility of the $i-V$ scans with a SAM of **VII** is given in Figure S1. This material is available free of charge via the Internet at http://pubs.acs.org.

JA0359815